Biochemical and Biophysical Research Communications 437 (2013) 199–204

Contents lists available at SciVerse ScienceDirect

Biochemical and Biophysical Research Communications

journal homepage: www.elsevier.com/locate/ybbrc

Crystallographic study of multi-drug resistant HIV-1 protease lopinavir complex: Mechanism of drug recognition and resistance

Zhigang Liu [a,b], Ravikiran S. Yedidi [a,c], Yong Wang [a], Tamaria G. Dewdney [a], Samuel J. Reiter [a], Joseph S. Brunzelle [d], Iulia A. Kovari [a], Ladislau C. Kovari [a,*]

[a] Department of Biochemistry and Molecular Biology, Wayne State University School of Medicine, Detroit, MI 48201, United States
[b] Division of Internal Medicine, Harbor Hospital, Baltimore, MD 21225, United States
[c] Experimental Retrovirology Section, HIV and AIDS Malignancy Branch, National Cancer Institute, National Institutes of Health, Bethesda, MD 20892, United States
[d] Life Sciences Collaborative Access Team and Department of Molecular Pharmacology and Biological Chemistry, Northwestern University, Feinberg School of Medicine, Chicago, IL 60611, United States

ARTICLE INFO

Article history:
Received 4 June 2013
Available online 18 June 2013

Keywords:
HIV-1 protease
Multi-drug resistance
X-ray crystallography
IC50
Lopinavir

ABSTRACT

Lopinavir (LPV) is a second generation HIV-1 protease inhibitor. Drug resistance has rapidly emerged against LPV since its US FDA approval on September 15, 2000. Mutations at residues 32I, L33F, 46I, 47A, I54V, V82A, I84V, and L90M render the protease drug resistant against LPV. We report the crystal structure of a clinical isolate multi-drug resistant (MDR) 769 HIV-1 protease (resistant mutations at residues 10, 36, 46, 54, 62, 63, 71, 82, 84, and 90) complexed with LPV and the *in vitro* enzymatic IC_{50} of LPV against MDR 769. The structural and functional studies demonstrate significant drug resistance of MDR 769 against LPV, arising from reduced interactions between LPV and the protease target.

1. Introduction

Although neither a cure nor vaccine is currently available for HIV infection [1], the success of highly active anti-retroviral therapy (HAART) has made it the treatment of choice against HIV viral replication since the mid 1990s [2]. Due to the absence of a proofreading function in reverse transcriptase under the pressure of drug selection [3], the drug resistance issue becomes increasingly important as it limits the efficacy of HAART.

Protease inhibitors are often included as one of the components of HAART. Currently, there are nine FDA approved HIV-1 protease inhibitors on the market. Most of these drugs contain a hydroxyethylene core and are peptidomimetic competitive inhibitors against the HIV-1 protease by mimicking the natural substrates [4–6]. Tipranavir, however, has a dihydropyrone ring as a central scaffold rather than a peptidomimetic hydroxyethylene core [7].

Lopinavir (LPV), approved by the FDA in 2000, is formulated with a low dose of ritonavir and is the first line treatment for pregnant women and pediatric patients. Although drug resistance is relatively less likely to develop against LPV compared to other HIV-1 protease inhibitors [8], resistance mutations, including 32I, 47A, 46I, L33F, I54V, V82A, I84V, and L90M, or combinations among L76V, M46I, and V82A in the protease, and A431V in gag [9] are responsible for reduced efficacy of LPV. In addition, it is found that the accumulation of mutations, including mutations of codons 82, 54, and 46, during prior protease inhibitor treatment facilitates the emergence of LPV resistant mutations [10].

Although crystal structures are available for LPV complexed with WT and limited drug resistant HIV-1 protease [11,12], structural data is not available for LPV complexed with an HIV-1 protease containing multiple drug resistant mutations, which is essential to understand the drug resistance mechanism.

To investigate the mechanism of LPV resistance, we chose a clinical isolate, MDR769 HIV-1 protease, as our study model. High resolution crystal structures of MDR769 HIV-1 protease showed an expanded active site cavity with mutations at positions 10, 36, 46, 54, 62, 63, 71, 82, 84, and 90 [13–15].

LPV was co-crystallized with MDR769 HIV-1 protease into space group $P4_1$, and the final structure was refined to 1.9 Å resolution. In addition, the *in vitro* IC_{50} of LPV against both WT and MDR769 HIV-1 protease was determined. The analysis of these structural and functional studies showed significant drug resistance of MDR HIV-1 protease against LPV, arising from the reduced interactions between LPV and MDR HIV-1 protease.

Abbreviations: MDR, multi-drug resistance; HAART, highly active anti-retroviral therapy; LPV, lopinavir; IC50, half maximal inhibitory concentration; RMSD, root mean square deviation.

* Corresponding author. Address: 540 E. Canfield Avenue, 4263 Scott Hall, Detroit, MI 48201, United States.
E-mail address: kovari@med.wayne.edu (L.C. Kovari).

0006-291X/$ - see front matter © 2013 Elsevier Inc. All rights reserved.
http://dx.doi.org/10.1016/j.bbrc.2013.06.027

2. Materials and methods

2.1. Protein purification and co-crystallization

The MDR769 HIV-1 protease was over expressed by using a T7 promoter expression vector in conjunction with the Escherichia coli host, BL21 (DE3) as described previously [16].

LPV was mixed with 2.5 mg/ml MDR769 HIV-1 A82T and diluted to 0.4 mM final concentration. The hanging drop vapor diffusion method was used to form the bi-pyramidal crystals with the MDR769 protease-LPV complex as described previously [6].

2.2. Data collection and crystallographic refinement

The diffraction data were collected at 0.972 Å wavelength at the Advanced Photon Source (APS) (LS-CAT 21), Argonne National Laboratory (Argonne, IL). Data were reduced to structure amplitudes with CrystalClear. The crystallographic statistics are shown in Table 1. Molecular replacement was performed with Molrep-autoMR in CCP4 [17] with a model previously solved in our lab. Initial refinements were calculated in the absence of LPV with Refmac5 [18]. The LPV molecule was built into the difference electron density maps processed with program COOT [19]. Crystallographic waters were added with ARP/wARP [20]. The structure was refined to resolution 1.9 Å with Refmac5. The final structure was checked using PROCHECK [21]. Images were generated in PyMol.

Table 1
Data collection and crystallographic refinement statistics.

Data collection	
Beam line	APS (LS-CAT 21)
Wavelength (Å)	0.972
Space group	*P41*
Cell dimension (Å) *a*, *b*, *c*	*a* = *b* = 43.82 *c* = 101.81
Resolution (Å)	33.21–1.50
R merge (%)[a]	8.0/51.5[b]
I/σ (*I*)	9.1/2.2
Redundancy	5.99/4.28
Completeness (%)	99.8/98.5
Unique reflection	30686
Refinement	
Resolution range (Å)	43.81–1.9
R work (%)[c]	19.7
R free (%)[d]	26
No. of protein atom	1514
No. of water molecule	222
B factor	
Whole molecules	21.672
Side chain (include water)	24.073
Main chain	18.669
Ligand	43.369
Solvent	30.638
RMSD	
Bond length	0.016
Bond angle	1.815
Ramachandran plot	
Favorable (%)	94.9
Additional (%)	5.1
Generous (%)	0
Forbidden (%)	0
PDB accession ID	4L1A

[a] $R\text{merge} = \Sigma hkl \Sigma i |I(hkl)i - \{I(hkl)\}| / \Sigma hkl \Sigma i I(hkl)i$, where $I(hkl)i$ is the intensity of an observation and $I(hkl)$ is the mean value for its unique reflection. Summations cover all reflections.

[b] The values after the hyphens indicate the highest resolution shell.

[c] $R\text{work} = \Sigma hkl |F(hkl)o - \{F(hk|/\Sigma hkl F(hkl)o$.

[d] *R* free was calculated the same way as *R* working, but with the reflections excluded from refinement. The *R* free set was chosen using default parameters in Refmac 5.

2.3. Analysis

PISA Server [22] was used to calculate the ligand binding energy in both MDR and WT HIV-1 protease LPV complexes. In addition, the hydrogen bonds that docked LPV were also analyzed by the PISA Server. WT and MDR complexes were superimposed based on protease residues 1–99 Cα and RMSD of Cα was analyzed with CCP4 Superpose Molecules. The solvent accessible area was calculated using CCP4 Accessible Surface Areas.

2.4. Enzyme assay

Inhibitory efficacy experiments were performed as described previously to determine the IC_{50} of LPV against MDR HIV-1 protease and WT HIV-1 protease [6].

3. Results

3.1. Inhibition studies of LPV against WT and MDR HIV-1 protease

The IC_{50} of LPV was determined against both WT (NL4-3) and MDR HIV-1 protease. Fluorescently labeled MA/CA substrate peptide was added to monitor the enzyme activity at different LPV concentrations.

The IC_{50} of LPV against WT and MDR769 HIV-1 protease was 1.24 ± 0.14 and 5.39 ± 0.225 nM, respectively. This result demonstrated a 4.34-fold drug resistance of MDR769 HIV-1 protease against LPV compared to WT HIV-1 protease. The free energy of binding (ΔG) as calculated by the PISA server is −26.1 and −16 kcal/mol for the WT and MDR 769 respectively; suggesting that the reduced efficacy of LPV against MDR 769 is due to a decrease in binding affinity.

3.2. Crystal structure of MDR769 HIV-1 protease LPV complex

LPV was co-crystallized with MDR769 HIV-1 protease into space group $P4_1$ and the final structure was refined to resolution 1.9 Å with Refmac5. In each asymmetric unit, there was one HIV-1 protease dimer, with two identical monomers consisting of 99 amino acids. In addition, 222 crystallographic water molecules were observed in the complex. The electron density maps demonstrated two orientations of bound LPV to the MDR HIV-1 protease. The two LPV orientations were related by a pseudo-2-fold symmetry, and there was minimal asymmetry for the two orientations of LPV as was the case for the WT HIV-1 LPV complexes. To simplify the analysis, LPV was fit into the electron density map in one orientation with occupancy of 0.5. The data collection and refinement statistics are shown in Table 1.

3.3. Fewer hydrogen bonds in MDR HIV-1 protease LPV complex

Six hydrogen bonds between LPV and MDR769, while seven were observed in the WT LPV complex (Fig. 1) [11]. In addition, the hydrogen bond length in the MDR769 LPV complex was longer than those seen in WT LPV complex (Table 2). Four out of the six hydrogen bonds in the MDR complex were also present in the WT LPV complex. Two new hydrogen bonds were observed in the MDR 769 LPV complex: N4 to Gly 27′ O and O3 to Asp 29′ N. Moreover, in the MDR 769 LPV complex, O4 formed a hydrogen bond only with Asn 25 ND2, while in the WT complex; O4 formed four hydrogen bonds with Asp 25/25′ OD1/OD2, which more firmly secured the position of LPV. The shift (2.5 Å) of O4 atom of LPV in the MDR complex compared to the WT complex lead to the dramatic hydrogen bond differences.

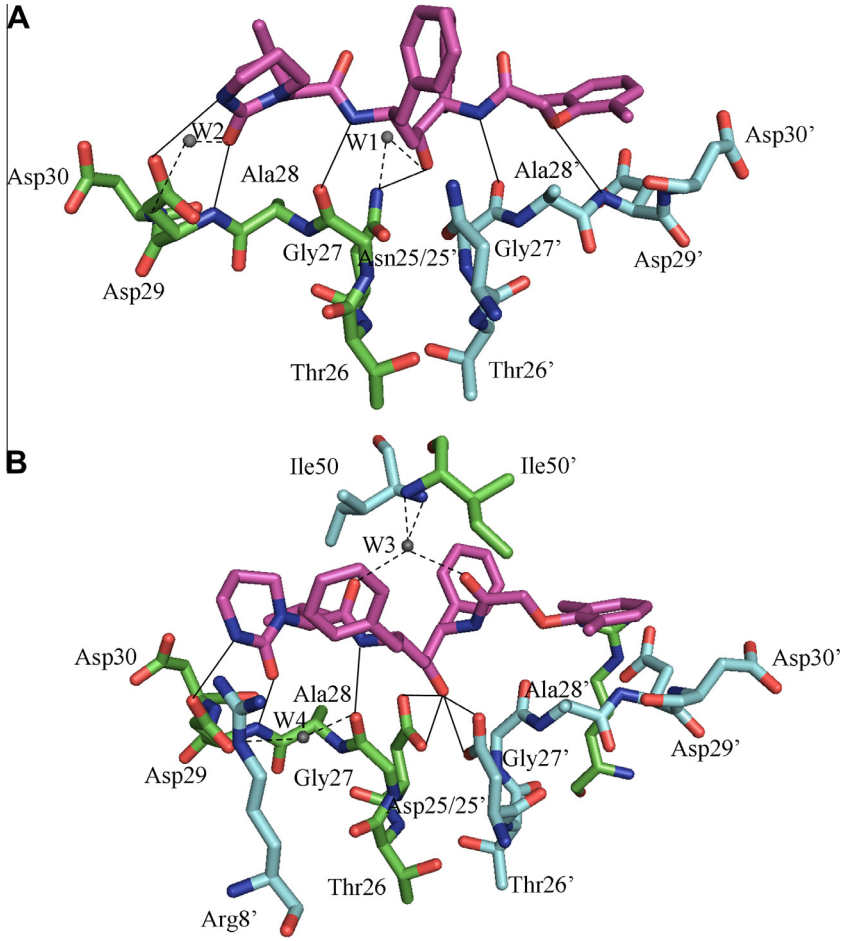

Fig. 1. Hydrogen bonds and crystallographic water molecules involved in LPV recognition and binding in both MDR 769 (Panel A) and WT (Panel B) complexes (2Q5K) [11]. LPV is shown in purple with stick model, and protease monomers are shown in green and cyan with stick model. The crystallographic water molecules are shown as grey sphere model. Hydrogen bonds between LPV and protease monomers are presented with solid line. The hydrogen bonds mediating substrate recognition via crystallographic water molecules are shown with dash line. (For interpretation of the references to color in this figure legend, the reader is referred to the web version of this book.).

Table 2
Hydrogen bonds involved in the LPV recognition.

Protein Atom	MDR LPV complex		WT LPV complex	
	LPV atom	Length (Å)	LPV atom	Length (Å)
Asp 29 OD1	N2	3.23	N2	2.97
Asp 29 N	O1	2.72	O1	2.74
Gly 27 O	N3	3.30	N3	3.00
Asp 25 OD1	O4	2.25	O4	2.81
Asp 25 OD2			O4	2.95
Asp 25′ OD1			O4	2.71
Asp 25′ OD2			O4	2.72
Gly 27′ O	N4	3.14		
Asp 29′ N	O3	3.30		

3.4. Fewer Van der Waals interactions in MDR HIV-1 protease LPV complex

Similar to hydrogen bonds, fewer Van der Waals interactions were found in the MDR 769 LPV complex compared to those in the WT LPV complex. In the MDR LPV complex, the ligand LPV, formed 14 and 16 Van der Waals interactions with protease monomer A and B respectively. In addition, Gly 49 from monomer A, Gly 49 and Leu 76 from monomer B were not involved in the Van der Waals interactions with LPV. In comparison, the amount of Van der Waals interactions in the WT complex was 15 and 18 respectively and Gly 49 from monomer A, Gly 49 and Leu 76 from monomer B were in direct contact with LPV.

3.5. Reduced surface area of LPV buried by MDR 769 HIV-1 protease

The surface area of LPV buried by the protease within the MDR 769 complex was also reduced compared to that in WT LPV complex, due to the reduced hydrogen bonds and Van der Waals interactions. In the MDR complex, 643.4 Å^2 of LPV was inaccessible to solvent, which made up 75.6% of the total surface area in contrast to 850.8 Å^2 surface area of LPV (91.3%) was buried by the protease in the WT complex [11]. This finding supports the enlarged active site cavity hypothesis leading to multi-drug resistance in the HIV-1 protease.

3.6. Crystallographic water molecules involved in LPV recognition to MDR 769 HIV-1 protease

Crystallographic water molecules participated in the ligand recognition in MDR HIV-1 protease LPV complex, as shown in Fig. 1. In the MDR 769 complex, water 1 (W1) bridged O4 from LPV and ND2 from Asn 25 (monomer A). In addition, water 2 (W2) bridged O1 from LPV and N from Asp 30 (monomer A) (Fig. 1 Panel A). Crystallographic water molecules with similar functions were also present in the WT HIV-1 protease LPV complex. However, these water molecules formed a more extensive network in the WT LPV complex than in MDR769 HIV-1 protease LPV complex (Fig. 1 Panel B) [11].

The characteristic crystallographic water W3, locating between the two protease flaps and LPV, was not seen in the MDR HIV-1 LPV

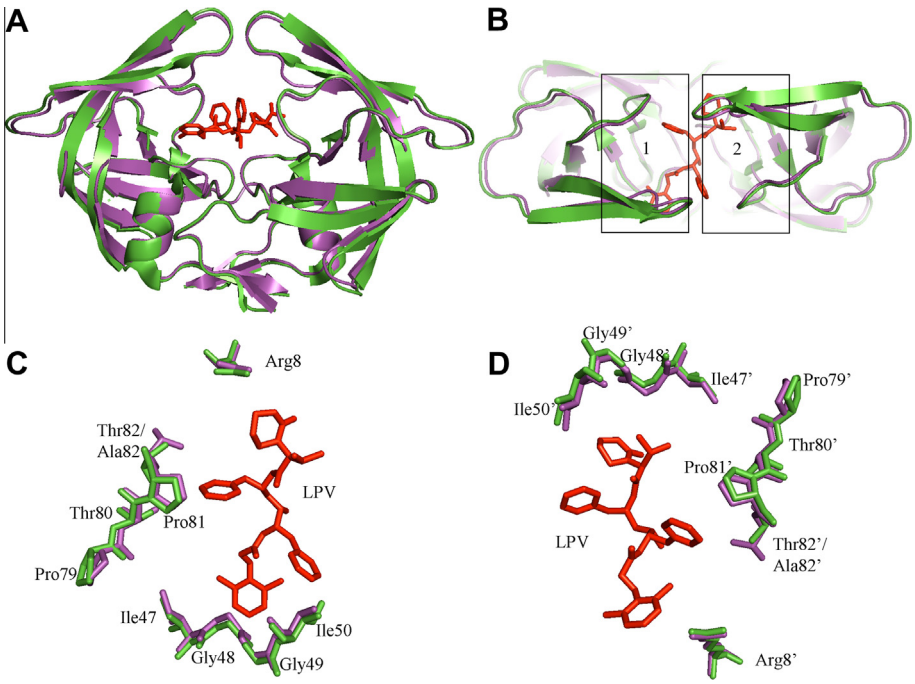

Fig. 2. Induced conformational changes of MDR HIV-1 protease upon binding of LPV. LPV is represented with red stick model. Apo-MDR HIV-1 protease (1TW7) [23] is shown in green color, while purple represents MDR 769 complexed with LPV. (A) Front view of the superposition of apo-MDR 769 and MDR 769 LPV complexes. (B) Top view of the superposition of apo-MDR 769 MDR 769 LPV complexes. (C) Conformational changes induced by LPV binding in the 80s loop, flap region and Arg 8 on monomer A, showing the details in box 1. (D) Conformational changes induced by LPV binding in the 80's loop, flap region and Arg 8 on monomer B, showing the details in box 2. (For interpretation of the references to color in this figure legend, the reader is referred to the web version of this book.)

complex. In the WT complex, this crystallographic water molecule bridged O2 and O5 from LPV with the amino group of Ile 50 in both monomers (Fig. 1 Panel B) [11]. The absence of the flap-ligand bridging water molecule may partially explain the wide open nature of the MDR 769 flaps as well as the relatively weaker binding energy of LPV to MDR 769.

3.7. Induced conformational changes of MDR HIV-1 protease upon LPV binding

Superimposition of MDR 769 LPV complex and apo-MDR 769 based on Cα revealed three high RMSD regions. First, residues 13–19, a surface loop connecting two β strands, did not contribute to the overall stability of the LPV complex despite the high RMDS. Second, residues 39–71 constituted four loops and four β strands. Three of these loops were on the surface of the protease, while the other one formed the tip of the flaps. The high RMSD of the flap tips gave rise to the slightly shorter flap distance of the MDR 769 LPV complex. Third, the last high RMSD region contained residues 79–83, which constituted the 80's loop of the MDR HIV-1 protease.

Due to the binding of LPV, the 80's loop was attracted towards the active site cavity, making more contacts than otherwise (Fig. 2 Panel B–D). In addition, the shift of the 80s loop slightly closed the lateral opening of the active site cavity, formed by residues 81, 82 (monomer A), 8′, 47′, 48′, 49′, 50′ (monomer B), and made it less likely for LPV to slip out of the active site cavity from the lateral opening (Fig. 2). As a result, the conformational changes of MDR HIV-1 protease favor LPV binding. However, the presence of LPV did not induce significant RMSD changes in the catalytic triplets of residues 25, 26, and 27.

3.8. Wide open flaps of MDR HIV-1 protease despite LPV binding

The flaps were wide open in the MDR 769 LPV complex. Contrary to the WT protease LPV complex, the binding of LPV did not close the flaps dramatically. The flap distance was measured from the Cα of Ile 50 in one monomer to the Cα of Ile 50 in the other monomer. The flap distance in the WT LPV complex was 5.9 Å [11] while in the apo MDR 769 protease, the flap distance was 12.2 Å. The flap distance in the MDR 769 LPV complex was 11.9 Å. The wide open flaps contribute to the weaker binding of LPV to MDR HIV-1 protease, making it easier for LPV to be released from the active site cavity.

3.9. Increased dimerization area of MDR HIV-1 protease induced by LPV binding

The MDR HIV-1 protease dimer was further stabilized by the binding of LPV compared to apo-MDR 769. In the absence of LPV, the MDR 769 dimerization area was 1330.9 Å^2. With LPV bound to MDR 769, the dimerization area increased by 7% to 1423.7 Å^2. In addition, the hydrogen bonds between the monomers increased from 23 in apo-MDR 769 to 28 in the MDR 769 LPV complex. Similarly, the salt bridges on the dimerization interface increased from 8 to 9 after the binding of LPV. However, the dimer interface area of the MDR 769 LPV complex was less than that of the WT HIV-1 protease LPV complex, considering the following parameters in WT complex: 1733.3 Å^2 interface area, 31 hydrogen bonds, and 10 salt bridges [11].

4. Discussion

4.1. Conserved Van der Waals interactions involving the 80's loop between WT and MDR 769 HIV-1 protease LPV complexes

Although there is a significant conformational change of the 80's loop between MDR 769 and WT HIV-1 protease LPV complexes, the Van der Waals interactions involving the 80's loop are conserved. Cγ of Pro 81 in monomer A moves 1.3 Å and Cγ of Pro 81 in monomer A moves 1.7 Å. However, due to the compensatory movement of LPV relative to the 80s loop, Cγ and Cβ of Pro 81

maintain similar Van der Waals interactions with LPV in both MDR and WT complexes (Fig. 3 Panel A and B).

In MDR 769 LPV complex, the Cγ, Cβ, and Cδ from Pro 81′ on chain B form Van der Waals interactions with C16 of LPV. Cγ2 of Val 82' on monomer B forms Van der Waals interactions with C16, C17, and C18 of LPV. In addition, Cβ of Pro 81 on monomer A forms Van der Waals interactions with C6 and C7 of LPV. Cγ of Pro 81 on monomer A forms Van der Waals interactions with C7 of LPV. Cγ2 of Val 82 on monomer A forms Van der Waals interactions with C6 and C7 of LPV. The Van der Waals interactions between the 80's loop and LPV in the WT and MDR 769 LPV complexes are shown in Table 3. Both the number and length of the Van der Waals interactions are conserved (Fig. 3 Panel A and B).

Table 3
Van der waal interactions involving 80s loop and Arg 8.

Protein atom	MDR LPV complex		WT LPV complex	
	LPV atom	Length (Å)	LPV atom	Length (Å)
Pro 81 Cβ	C6	3.6	C7	3.9
	C7	3.5	C8	4.2
Pro 81 Cγ	C7	3.8	C8	3.8
Thr 82/Val 82 Cγ1	C5	3.8	C6	3.7
	C6	4.2	C7	4.0
Arg 8	C32	3.8		
	C33	3.2		
	C34	3.7		
	C35	3.9		
Pro 81′ Cβ[a]	C17	3.6	C16	3.8
Pro 81′ Cγ	C17	3.3	C16	3.8
	C18	4.0		
Pro 81′ Cδ			C16	4.0
Thr 82′/Val 82′ Cγ1	C16	3.6	C16	4.1
	C21	3.8	C17	3.9
			C18	4.0
Arg 8′ NH2	N2	3.7	N2	3.5
	C1	3.4	C18	4.1

[a] The residues denoted by the symbol ′ indicate those from monomer B, while the residues without symbol ′ are those from monomer A.

4.2. Different Van der Waals interactions involving Arg 8 between WT and MDR HIV-1 protease LPV complexes

The analysis of Arg 8 in the LPV complex reveals surprising aspects of LPV binding in MDR HIV-1 protease. The amino group of Arg 8 on monomer A forms four Van der Waals interactions with C32, C33, C34, and C35 of LPV in MDR 769 LPV complex, while no Van der Waals interactions are observed between Arg 8 on monomer A and LPV in the WT complex (Fig. 3 Panel C). On the other hand, the Arg 8′ NH_2 on monomer B forms two Van der Waals interactions with LPV in both MDR and WT LPV complexes (Fig. 3 Panel D). This result indicates that in MDR 769 LPV complex, the Arg 8 from both monomers participates in the binding of LPV, making it less likely for LPV to escape from the active site cavity via the lateral opening. Since the flap opening is the only outlet of the active site cavity, it may indicate a significant contribution to the drug resistance by the wide open flaps in MDR 769 LPV complex.

The differences in interactions between Arg 8 on monomer A and LPV may be explained by the shift of LPV within the MDR 769 active site cavity. In the MDR 769 LPV complex, the ligand LPV is shifted as a whole entity by 2.5 Å towards the Arg 8 on monomer A, according to the distance of O4 atom of LPV in two different complexes.

4.3. Conformational changes of LPV between WT and MDR HIV-1 complexes

In addition to the conformational changes of the protease and the subsequent the LPV-protease interactions, major conformational changes are also found in LPV after the binding, despite

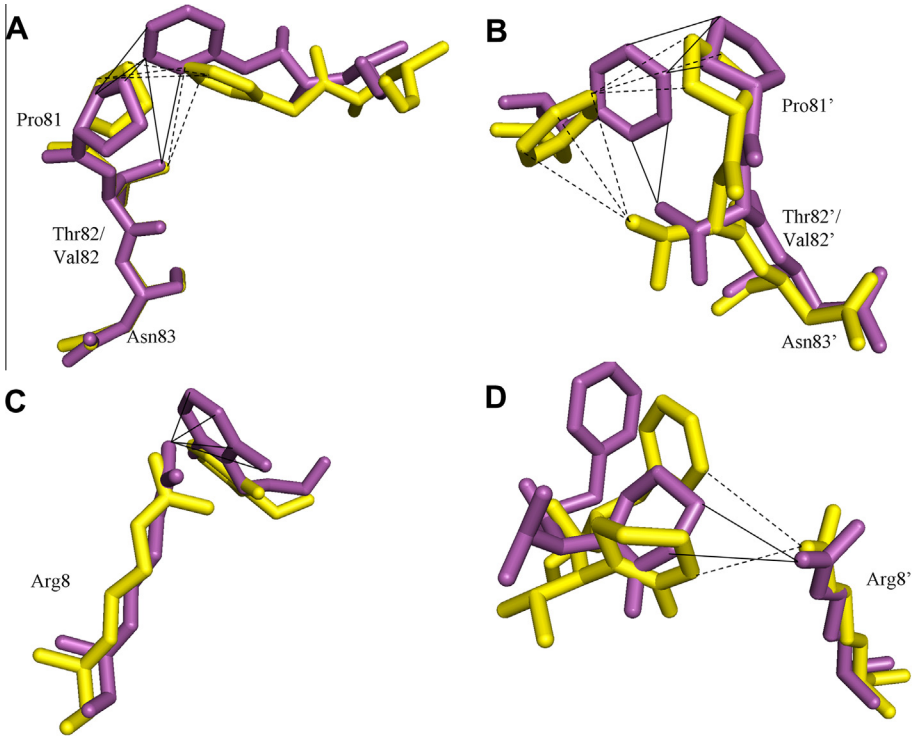

Fig. 3. Van der Waals interactions between LPV and HIV-1 protease. MDR 769 LPV complex is shown in purple and WT LPV complex is shown in yellow. The Van der Waals interactions between LPV and MDR 769 are shown in solid line, while those between LPV and WT are shown in dash line. (A) Van der Waals interactions between LPV and the 80's loop of monomer A. (B) Van der Waals interactions between LPV and the 80's loop of monomer B. (C) Van der Waals interactions between LPV and Arg 8 on monomer A. (D) Van der Waals interactions between LPV and Arg 8′ on monomer B. (For interpretation of the references to color in this figure legend, the reader is referred to the web version of this book.)

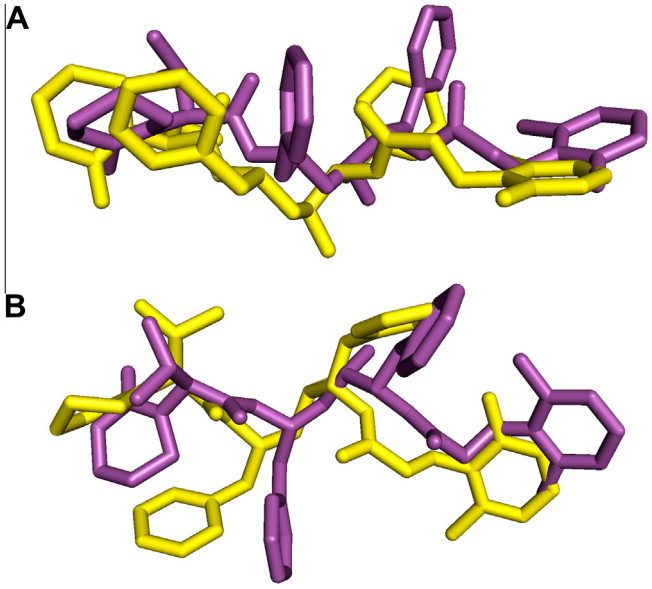

Fig. 4. Conformational changes (Panel A front view, Panel B top view) of LPV in MDR and WT HIV-1 protease LPV complexes. LPV in MDR HIV-1 protease is shown in purple and LPV in WT HIV-1 protease is shown in yellow. (For interpretation of the references to color in this figure legend, the reader is referred to the web version of this book.)

the relative rigidity of LPV compared to the natural substrate peptides. These conformational changes in LPV, in turn, modify the interactions between the ligand and receptor. Although the conformation of LPV backbone is conserved between two complexes, the side chains, especially the ring structures, are rotated significantly to adjust the changes in protease (Fig. 4).

4.4. LPV analogs with expanded side chains may restore the binding affinity

The studies of MDR 769 complex may provide some novel strategies for HIV-1 protease inhibitor design to overcome the drug resistance issue. The loss of interactions between LPV and MDR HIV-1 protease is caused by two independent factors. First, the active site cavity of MDR HIV-1 protease is enlarged relative to WT HIV-1 protease. Second, the rotation of the side chains of LPV reduces the interaction further. As a result, we may restore the LPV binding affinity by expanding the LPV side chains to accommodate the expanded active site cavity.

Acknowledgments

This research was supported by the National Institutes of Health Grant AI65294 and the American Foundation for AIDS Research (106457-34-RGGN).

References

[1] R.T. Schooley, J.W. Mellors, No cure yet for HIV-1, but therapeutic research presses on, J. Infect. Dis. 195 (2007) 770–772.
[2] G. Barbaro, A. Lucchini, G. Barbarini, Highly active antiretroviral therapy in HIV-associated pulmonary hypertension, Minerva Cardioangiol. 53 (2005) 153–154.
[3] Y. Takeuchi, T. Nagumo, H. Hoshino, Low fidelity of cell-free DNA synthesis by reverse transcriptase of human immunodeficiency virus, J. Virol. 62 (1988) 3900–3902.
[4] J.A. Partaledis, K. Yamaguchi, M. Tisdale, E.E. Blair, C. Falcione, B. Maschera, R.E. Myers, S. Pazhanisamy, O. Futer, A.B. Cullinan, et al., In vitro selection and characterization of human immunodeficiency virus type 1 (HIV-1) isolates with reduced sensitivity to hydroxyethylamino sulfonamide inhibitors of HIV-1 aspartyl protease, J. Virol. 69 (1995) 5228–5235.
[5] A.K. Patick, H. Mo, M. Markowitz, K. Appelt, B. Wu, L. Musick, V. Kalish, S. Kaldor, S. Reich, D. Ho, S. Webber, Antiviral and resistance studies of AG1343, an orally bioavailable inhibitor of human immunodeficiency virus protease, Antimicrob. Agents Chemother. 40 (1996) 292–297.
[6] Z. Liu, R.S. Yedidi, Y. Wang, T.G. Dewdney, S.J. Reiter, J.S. Brunzelle, I.A. Kovari, L.C. Kovari, Insights into the mechanism of drug resistance: X-ray structure analysis of multi-drug resistant HIV-1 protease ritonavir complex, Biochem. Biophys. Res. Commun. 431 (2013) 232–238.
[7] Y. Wang, Z. Liu, J.S. Brunzelle, I.A. Kovari, T.G. Dewdney, S.J. Reiter, L.C. Kovari, The higher barrier of darunavir and tipranavir resistance for HIV-1 protease, Biochem. Biophys. Res. Commun. 412 (2011) 737–742.
[8] D.J. Kempf, M.S. King, B. Bernstein, P. Cernohous, E. Bauer, J. Moseley, K. Gu, A. Hsu, S. Brun, E. Sun, Incidence of resistance in a double-blind study comparing lopinavir/ritonavir plus stavudine and lamivudine to nelfinavir plus stavudine and lamivudine, J. Infect. Dis. 189 (2004) 51–60.
[9] R.J. Gifford, T.F. Liu, S.Y. Rhee, M. Kiuchi, S. Hue, D. Pillay, R.W. Shafer, The calibrated population resistance tool: standardized genotypic estimation of transmitted HIV-1 drug resistance, Bioinformatics 25 (2009) 1197–1198.
[10] H. Mo, M.S. King, K. King, A. Molla, S. Brun, D.J. Kempf, Selection of resistance in protease inhibitor-experienced, human immunodeficiency virus type 1-infected subjects failing lopinavir- and ritonavir-based therapy: mutation patterns and baseline correlates, J. Virol. 79 (2005) 3329–3338.
[11] G.S. Reddy, A. Ali, M.N. Nalam, S.G. Anjum, H. Cao, R.S. Nathans, C.A. Schiffer, T.M. Rana, Design and synthesis of HIV-1 protease inhibitors incorporating oxazolidinones as P2/P2' ligands in pseudosymmetric dipeptide isosteres, J. Med. Chem. 50 (2007) 4316–4328.
[12] K.G. Saskova, M. Kozisek, M. Lepsik, J. Brynda, P. Rezacova, J. Vaclavikova, R.M. Kagan, L. Machala, J. Konvalinka, Enzymatic and structural analysis of the I47A mutation contributing to the reduced susceptibility to HIV protease inhibitor lopinavir, Protein Sci. 17 (2008) 1555–1564.
[13] R.S. Yedidi, G. Proteasa, J.L. Martinez, J.F. Vickrey, P.D. Martin, Z. Wawrzak, Z. Liu, I.A. Kovari, L.C. Kovari, Contribution of the 80s loop of HIV-1 protease to the multidrug-resistance mechanism: crystallographic study of MDR769 HIV-1 protease variants, Acta Crystallogr. D Biol. Crystallogr. 67 (2011) 524–532.
[14] Z. Liu, Y. Wang, J. Brunzelle, I.A. Kovari, L.C. Kovari, Nine crystal structures determine the substrate envelope of the MDR HIV-1 protease, Protein J. 30 (2011) 173–183.
[15] Z. Liu, Y. Wang, R.S. Yedidi, T.G. Dewdney, S.J. Reiter, J.S. Brunzelle, I.A. Kovari, L.C. Kovari, Conserved hydrogen bonds and water molecules in MDR HIV-1 protease substrate complexes, Biochem. Biophys. Res. Commun. 430 (2013) 1022–1027.
[16] T.G.D. Yong Wang, Zhigang Liu, Samuel J. Reiter, Joseph S. Brunzelle, Iulia A. Kovari, Ladislau C. Kovari, Higher desolvation energy reduces molecular recognition in multi-drug resistant HIV-1 protease, Biology 1 (2011) 81–93.
[17] The CCP4 suite: programs for protein crystallography, Acta Crystallogr. D Biol. Crystallogr. 50 (1994) 760–763.
[18] G.N. Murshudov, A.A. Vagin, E.J. Dodson, Refinement of macromolecular structures by the maximum-likelihood method, Acta Crystallogr. D Biol. Crystallogr. 53 (1997) 240–255.
[19] P. Emsley, K. Cowtan, Coot: model-building tools for molecular graphics, Acta Crystallogr. D Biol. Crystallogr. 60 (2004) 2126–2132.
[20] V.S. Lamzin, K.S. Wilson, Automated refinement of protein models, Acta Crystallogr. D Biol. Crystallogr. 49 (1993) 129–147.
[21] A.A. Vaguine, J. Richelle, S.J. Wodak, SFCHECK: a unified set of procedures for evaluating the quality of macromolecular structure-factor data and their agreement with the atomic model, Acta Crystallogr. D Biol. Crystallogr. 55 (1999) 191–205.
[22] E. Krissinel, K. Henrick, Inference of macromolecular assemblies from crystalline state, J. Mol. Biol. 372 (2007) 774–797.
[23] P. Martin, J.F. Vickrey, G. Proteasa, Y.L. Jimenez, Z. Wawrzak, M.A. Winters, T.C. Merigan, L.C. Kovari, "Wide-open" 1.3 A structure of a multidrug-resistant HIV-1 protease as a drug target, Structure 13 (2005) 1887–1895.